ISSN 1063-7834, Physics of the Solid State, 2015, Vol. 57, No. 6, pp. 1201–1205. © Pleiades Publishing, Ltd., 2015.
Original Russian Text © S.V. Mel'nikova, N.M. Laptash, 2015, published in Fizika Tverdogo Tela, 2015, Vol. 57, No. 6, pp. 1180–1184.

PHASE TRANSITIONS

Optical Studies of the (T–x) Phase Diagram of Oxyfluoride $(NH_4)_2MoO_2F_4$–$Rb_2MoO_2F_4$ Solid Solutions

S. V. Mel'nikova[a, *] and N. M. Laptash[b]

[a] *Kirensky Institute of Physics, Siberian Branch of the Russian Academy of Sciences, Akademgorodok 50–38, Krasnoyarsk, 660036 Russia*

[b] *Institute of Chemistry, Far-Eastern Branch of the Russian Academy of Sciences, pr. Stoletiya Vladivostoka 159, Vladivostok, 690022 Russia*

**e-mail: msv@iph.krasn.ru*

Received December 15, 2014

Abstract—Single crystals of solid solutions $(NH_4)_{2-x}Rb_xMoO_2F_4$ (including individual complex $Rb_2MoO_2F_4$) have been grown and studied using polarization–optical methods. The birefringence $\Delta n(T)$ has been measured in the temperature range of 100–400 K. The complete (T–x) phase diagram has been constructed.

DOI: 10.1134/S1063783415060256

1. INTRODUCTION

The classical structure of oxyfluorides with the empirical formula $A_2MO_2F_4$ ($A = NH_4$, Rb; M = Mo, W) consists of isolated polar octahedral groups $[MO_2F_4]^{2-}$ and cations A, the half of which is pinned on the symmetry planes. The polarity of MO_2F_4 complexes is attractive due to the possibility of obtaining new functional noncentrosymmetric materials with a wide transparency range. However, most of the compounds crystallize in centrosymmetric space groups due to orientation disordering structural elements. During cooling, these materials undergo different variants of the ordering of structural groups as a result of the phase transition (PT) at a temperature T_1.

Ammonia compounds $(NH_4)_2MoO_2F_4$ and $(NH_4)_2WO_2F_4$, despite close ionic radii of Mo and W, differ in many parameters, including the physical origin of distorted phases. In $(NH_4)_2WO_2F_4$, during the ferroelastic transition ($T_{1\uparrow} = 202$ K) with thermal hysteresis $\delta T_1 \approx 6$–12 K ($Cmcm \longleftrightarrow P\bar{1}$), atoms O and F are completely ordered, and the ammonia groups are ordered partially [1]. In $(NH_4)_2MoO_2F_4$, during the antiferroelectric [2] transition ($T_{1\uparrow} = 267.8$ K) with $\delta T_1 \approx 0.6$ K ($Cmcm \longleftrightarrow Pnma$), ligands are ordered partially, and the ammonia groups are ordered completely with the formation of hydrogen bonds of the N–H···F(0) type [3]. In $Rb_2MoO_2F_4$ ($Cmcm$, $Z = 4$, $a = 5.972$ Å, $b = 14.273$ Å, $c = 7.084$ Å), at room temperature, atoms F and O are ordered partially [4]. According to the optical studies [5, 6], the first-order phase transition at T_1 in ammonia crystals is accompanied by significant anomalies in the birefringence with significantly different magnitudes. In $(NH_4)_2MoO_2F_4$, the anomalous part of the birefringence is two times larger than that in $(NH_4)_2WO_2F_4$, which can be related to different mechanisms of structural distortions [1, 3]. The compound with atomic cation $Rb_2MoO_2F_4$ was not studied by optical methods, but it is found to undergo a second-order PT ($Cmcm \longleftrightarrow P\bar{1}$) [7]. Above-mentioned $A_2MO_2F_4$ crystals demonstrate one more specific temperature $T_2 \approx 180$–200 K at which there are additional anomalies of the heat capacity [5, 6] and the birefringence [5, 6], which are do not related to changes in the symmetry. The origin of these anomalies is not understood, although the anomalies in $(NH_4)_2WO_2F_4$ [9] are explained by additional ordering of ammonia groups. To reveal the role of structural complexes $[NH_4]$ and $[MO_2F_4]$ in phase transitions at T_1 and T_2, it is interesting to study materials with atomic cation ($Rb_2MoO_2F_4$) and also the influence of gradual substitution $NH_4 \longrightarrow Rb$. The (T–x) phase diagram of solid solutions $(NH_4)_{2-x}Rb_xMoO_2F_4$ was studied in [7] by means of thermophysical measurements only in region $x = 0$–1. It was shown that these compounds undergo PT without changing crystal system ($Cmcm \longleftrightarrow Pnma$).

In this work, we have grown single crystals of solid solutions $(NH_4)_{2-x}Rb_xMoO_2F_4$ ($x = 0.52$, 0.84, 1.01, 1.50, 1.76), $(NH_4)_2MoO_2F_4$ ($x = 0$), and $Rb_2MoO_2F_4$ ($x = 2$). The techniques of growing and determining the composition of solid solution single crystals were described in [7]. The grown single crystals were studied by the polarization–optical methods; their birefringence $\Delta n(T)$ was measured in the temperature range of 100–400 K, and the complete (T–x) phase diagram of the solid solutions was constructed. The experiments were performed on the basis of an

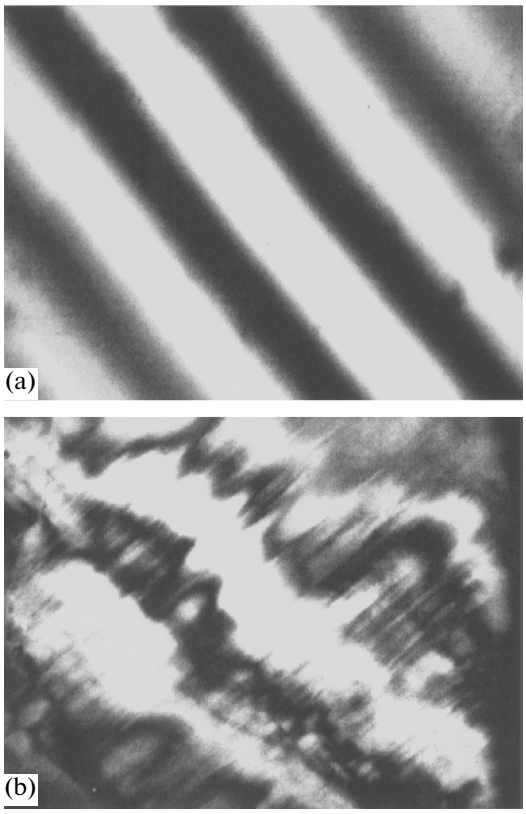

Fig. 1. Visualization of stripe twins in the (010) and (001) plates of the $Rb_2MoO_2F_4$ crystal with the use of a Berek compensator: (a) clear compensation band at $T = 260$ K and (b) smearing of the bands at $T = 250$ K.

Axioskop-40 polarization microscope, using a Linkam LTS 350 temperature chamber. The birefringence was measured by the Berek (Leica) compensator method with an accuracy of ±0.0001.

2. EXPERIMENTAL RESULTS

The habit and the arrangement of crystallographic axes of grown single-crystal $(NH_4)_{2-x}Rb_xMoO_2F_4$ solid solutions are the same for all x and coincide with the external parameters $(NH_4)_2MoO_2F_4$ [6].They are prismatic crystals with the elongation along [100] and perfect cleavage plane (010). The [010] crystallographic direction is directed along the short size of the crystal, as well as in the tungsten and molybdenum compounds [5, 6], and the [001] direction is directed along the average size of the prism. The refractive index ellipsoid (optical indicatrix) of the $(NH_4)_2MoO_2F_4$ crystals of all compositions ($x = 0$–2) at room temperature has the shape and position similar to those observed in $(NH_4)_2MoO_2F_4$ [6]: the optical axes lay in the (100) plane, and the angle of optical axes is close to 45°.

The observations in the polarized light showed that the plates of three orthogonal directions with compositions $x = 0$–1.5 demonstrate, in the temperature range of 100–400 K, an even and direct extinction that is characteristic of the orthorhombic symmetry [6]. However, the studies of $Rb_2MoO_2F_4$ ($x = 2$) reveal a different pattern. On cooling below a temperature of 280 K, optical inhomogeneities form in the (100) samples. They are observed as asterisks against the dark background in the extinction position. Below $T_1 = 255$ K, this pattern is imposed by a system of small striated twins with "floating" extinction. Striated twins are well observed in the (001) plates below $T_1 = 225$ K when the Berek compensator is introduced (Fig. 1). The photography shows a "smearing" of interference fringes of the compensator at twin boundaries. The (010) samples do not demonstrate clear extinction below $T = 255$ K and demonstrates "smearing" of the compensation bands. Unfortunately, the composition with $x = 1.76$ was studied only using the (010) growth plates because of their very small thickness (~50–60 μm), but the good extinction and clear compensation bands over the entire temperature range count in favor of the orthorhombic symmetry of the crystal. No any additional changes in this picture at temperatures near T_2 are observed.

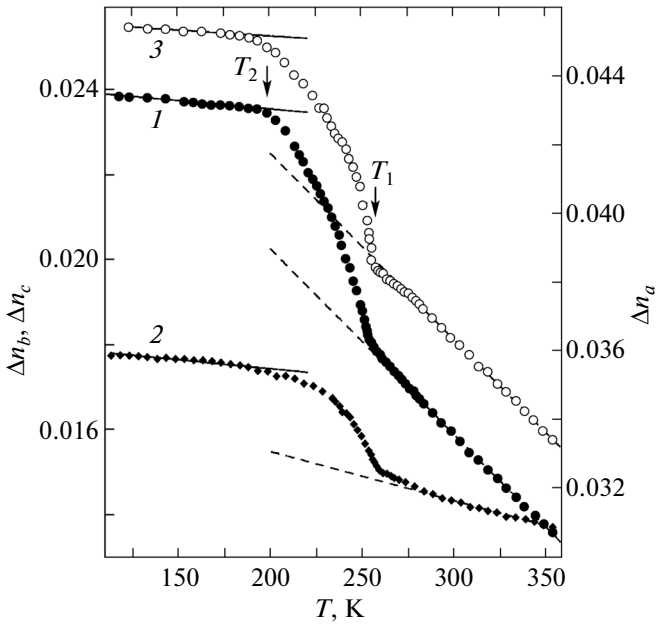

Fig. 2. Temperature dependences of the birefringence of $Rb_2MoO_2F_4$: (*1*) $\Delta n_a(T)$, (*2*) $\Delta n_b(T)$, and (*3*) $\Delta n_c(T)$.

The results of studying the temperature dependences of birefringences Δn_a, Δn_b, and Δn_c of the $Rb_2MoO_2F_4$ ($x = 2$) crystal are shown in Fig. 2. At room temperature, the birefringence has the maximum value ($\Delta n_a = 0.033$) as the light propagates along the [100] direction and the minimum value ($\Delta n_b = 0.014$) as the light propagates along the [010] direction. As the light is directed along [001], the optical anisotropy of the crystal is $\Delta n_c = 0.019$. The tempera-

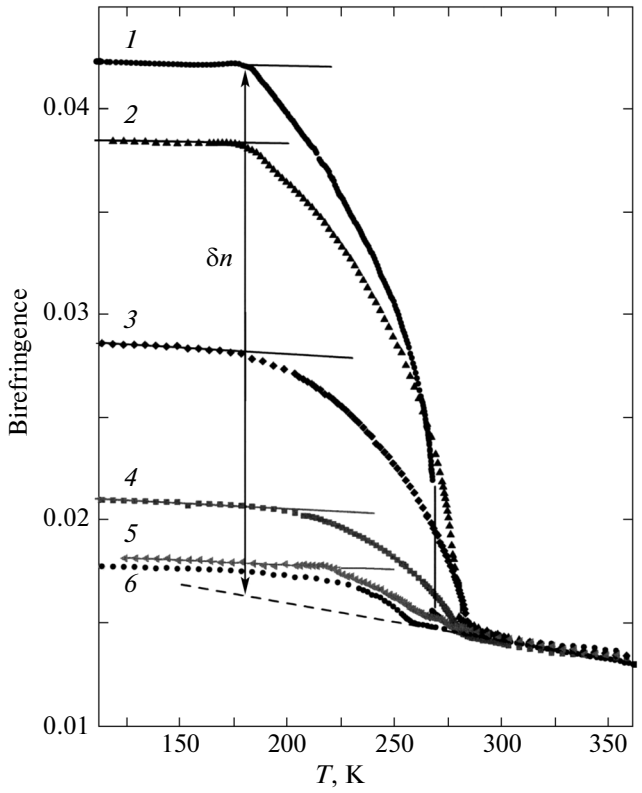

Fig. 3. Temperature dependences of the birefringence $\Delta n_b(T)$ of $(NH_4)_{2-x}Rb_xMoO_2F_4$ crystals with $x =$ (*1*) 0, (*2*) 0.52, (*3*) 1.01, (*4*) 1.5, (*5*) 1.76, and (*6*) 2.

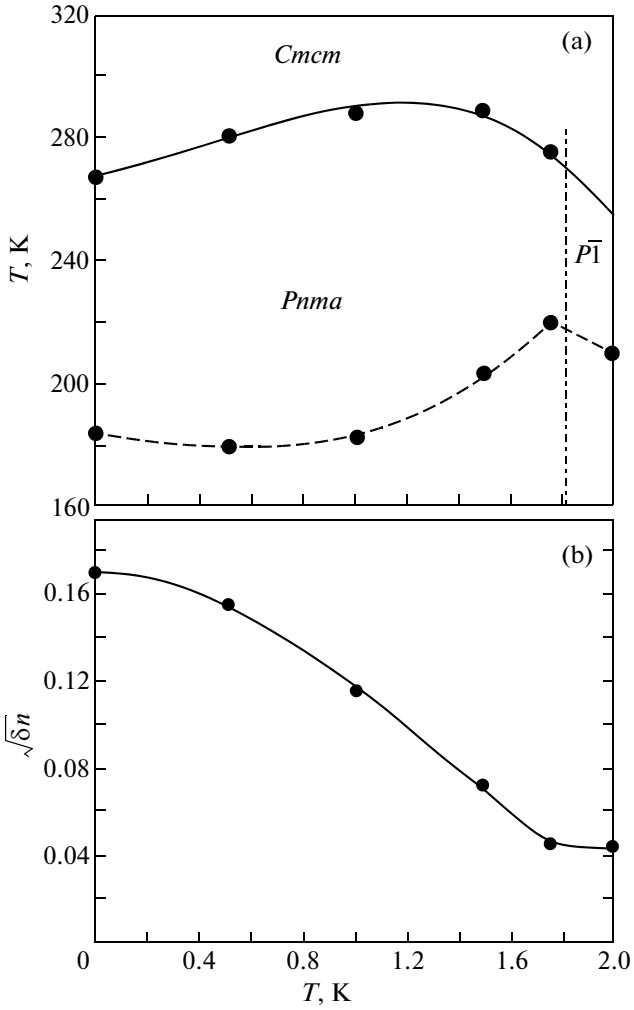

Fig. 4. (a) Phase $(T - x)$ diagram of $(NH_4)_{2-x}Rb_xMoO_2F_4$ solid solutions and (b) dependence $\sqrt{\delta n}\,(x) \propto \eta(x)$ near the temperature T_2.

ture dependences of these optical characteristics of the $Rb_2MoO_2F_4$ crystal are linear in the range of 370–280 K, and insignificant deviations from linearity are observed at 280–255 K. During further cooling, birefringences $\Delta n_{a,b,c}$ smoothly increase, thus forming two anomalies in $\Delta n_i(T)$ at $T_1 = 255$ K and $T_2 \approx 200$ K. At temperatures below T_2, dependence $\Delta n_i(T)$ becomes linear. The shape of the anomaly in the birefringence near T_2 is dependent on the rate of varying temperature and direction of the thermal process. The bend of curve $\Delta n_i(T)$ is most clearly observed at T_2 during slow heating (Fig. 2, curve *1*).

To study the (*T*–*x*) phase diagram of the solid solutions, we performed the temperature measurements of Δn_b for different *x*. This choice of the sample orientation is explained by two reasons: (1) the crystals grow with the developed (010) face, which gives the possibility to use the growth plate; and (2) at high temperatures, the values and the temperature behaviors of birefringence $\Delta n_b(T)$ are the same in crystals $(NH_4)_2WO_2F_4$ [5], $(NH_4)_2MoO_2F_4$ [6], and $Rb_2MoO_2F_4$ (Fig. 2, curve *2*). Figure 3 shows temperature dependences $\Delta n_b(T)$ of the $(NH_4)_{2-x}Rb_xMoO_2F_4$ solid solutions. It is seen that, during substitution $NH_4 \longrightarrow Rb$, the anomaly in the birefringence decreases gradually and very significantly (by a factor of more than 10) at temperatures lower than transition temperature T_1. In this case, at temperature T_2, dependences $\Delta n_b(T)$ are flattens out at all *x*. The bend in $\Delta n_b(T)$ at $T = T_2$ is observed more clear during heating (Fig. 3, curves *1*, *2*, *5*). Specific temperature points T_1 and T_2 are changed from composition to composition, forming the (*T*–*x*) phase diagram (Fig. 4a). The left part of the diagram completely coincides with that obtained in [7] during studying the heat capacity.

3. DISCUSSION OF THE RESULTS

The polarization-optical studies of the single-crystal samples of different orientations show that the plate with compositions $x = 0$–1.76 demonstrate the direct extinction at temperatures $T < T_1$, as is the case at room temperature. This fact counts in favor of the orthorhombic symmetry of crystals at low tempera-

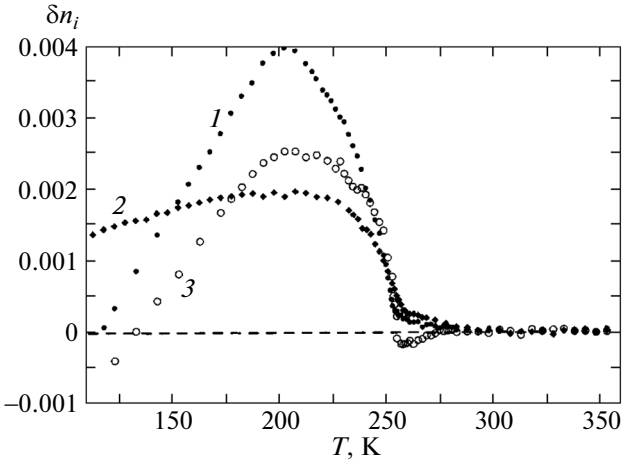

Fig. 5. Temperature dependences of the anomalous part of the birefringence in $Rb_2MoO_2F_4$: (*1*) $\delta n_a(T)$, (*2*) $\delta n_b(T)$, and (*3*) $\delta n_c(T)$.

tures as is the case in $(NH_4)_2MoO_2F_4$ [6]. In $Rb_2MoO_2F_4$ ($x = 2$) at $T < T_1$, there is a small (~1 μm) twin structure with floating position of the extinction in cut (100) and also unclear extinction in the (010) and (001) plates. This fact indicates a low symmetry of the crystal at temperatures $T < T_1$. Thus, similar to $(NH_4)_2WO_2F_4$ [5], crystal $Rb_2MoO_2F_4$ at T_1 undergoes the ferroelastic PT to the triclinic phase (*Cmcm* ⟷ $P\bar{1}$), which agrees with [7]. From the (T–x) phase diagram (Fig. 4a), it follows that the transition occurs in very narrow region near $x = 2$. In the entire remaining region of values x at T_1, the symmetry change *Cmcm* ⟷ *Pnma* takes place, as is the case in $(NH_4)_2MoO_2F_4$. Similar picture was observed in the studies of a gradual substitution of the central atom in $(NH_4)_2W_{1-x}Mo_xO_2F_4$ solid solutions [8]. It was shown that the antiferroelectric state formed at low temperatures and molybdenum concentrations $x > 0.3$ is most stable, i.e., energetically favorable. And only in a narrow region of values $x < 3$, this solid solution undergoes the phase transition to the ferroelastic state.

Figure 5 shows the temperature dependences of the anomalous part of the birefringence $\delta n_i(T)$ for three directions of light propagation in $Rb_2MoO_2F_4$ obtained by subtracting the extrapolated temperature run of the birefringence of the initial phase (dashed lines) from experimental curves $\Delta n_i(T)$ (Fig. 2). It is seen that, in the range $T - T_1 \approx 25$ K, this crystal demonstrates pre-transition phenomena (similar to those in $(NH_4)_2WO_2F_4$) which are 10% of the maximum value of the anomaly, and this fact is likely an indirect indicator of the ferroelastic nature of PT at T_1.

At $T_1 = 255$ K, the main anomaly $\delta n_i(T)$ is characteristic of a second-order PT. We should focus our attention on the fact that the value of the anomalous part of the birefringence (δn_i) in the rubidium-containing crystal is much lower than that in the ammonia compounds [5, 6]. Thus, near a temperature $T \geq T_2$, the sum of anomalous parts of the birefringence $\sum|\delta n_i|$ is 0.054 for the $(NH_4)_2WO_2F_4$ crystal [5] and 0.098 for the $(NH_4)_2MoO_2F_4$ crystal [6]; in the present work, we obtained $\sum|\delta n_i| = 0.008$ for the rubidium oxyfluoride. In this case, according to [1, 3], at temperatures lower than T_1, the ammonia groups are partially ordered in $(NH_4)_2WO_2F_4$ and completely ordered in $(NH_4)_2MoO_2F_4$. Thus, there is a correlation between the degree of ordering the ammonia cation and the value of the anomaly in the birefringence accompanying PT.

In $Rb_2MoO_2F_4$, against the background of a weak (as compared to that of the ammonia crystals [5, 6]) anomaly at T_1, a second feature $\delta n_i(T)$ is more clearly observed near T_2 (Fig. 5) whose value is comparable to the first anomaly. It should be noted that the additional changes in the optical anisotropy related to T_2 are almost the same in magnitude in all three $A_2MO_2F_4$ crystals.

The anomalous part of the birefringence measured in the orthorhombic setting is proportional to the squared transition parameter and, because of this, characterizes its temperature dependence: $\delta n(T) \propto \eta^2(T)$. Taking into account this correlation, we can determine the temperature behavior of the transition parameter $\eta(T)$ or $\eta(x)$ in the range $T_1 > T > T_2$. Figure 4b shows dependence $\sqrt{\delta n}(x) \propto \eta(x)$ obtained from Fig. 3 at temperatures slightly higher than T_2. It is seen that, during substitution $NH_4 \longrightarrow Rb$, the transition parameter varies linearly in the range $0.4 < x < 1.75$. In the reminder of values of x, the replacement of ammonia with rubidium does not substantially change the birefringence. According to [3], the ammonia tetrahedra occupy two crystallographically different position in the $(NH_4)_2MoO_2F_4$ structure, and they form or do not form hydrogen bonds at temperatures lower than T_1. Because of this, based on the shape of the curve in Fig. 4b, we suggest that different positions of the molecules are occupied inhomogeneously during the gradual substitution $NH_4 \longrightarrow Rb$. The, ammonia that has not hydrogen bond with the octahedral is the first to be replaced. The electron polarizability varies insignificantly. In the central part of the phase diagram, the substitution occurs in the position that gives a strong response in the optical properties due to the existence of the hydrogen bond. Substitution $NH_4 \longrightarrow Rb$ also slightly influence on the optical properties at large values of x.

4. CONCLUSIONS

The performed polarization-optical studies and the measurements of the temperature dependences of the

birefringence of the solid solution $(NH_4)_{2-x}Rb_xMoO_2F_4$ single crystals, including individual complexes $(NH_4)_2MoO_2F_4$ ($x = 0$) and $Rb_2MoO_2F_4$ ($x = 2$), showed that all compositions have similar sequence of two phase transitions. At temperatures lower than PT temperature T_1, the plates of three orthogonal directions with compositions $x = 0$–1.76 demonstrated the smooth extinction in polarized light; twins were not observed; i.e., the crystals were retained in the orthorhombic system like in $(NH_4)_2MoO_2F_4$ (*Cmcm* ⟷ *Pnma*). In $Rb_2MoO_2F_4$ ($x = 2$) at $T < T_1$, there is a fine twin structure indicating PT to the triclinic phase (*Cmcm* ⟷ $P\bar{1}$), as is the case in $(NH_4)_2WO_2F_4$. Thus, at low temperatures, the antiferroelectric state formed in the solid solutions over wide range of rubidium concentrations ($x = 0$–1.8) is most stable; i.e., it is energetically favorable. During substitution $NH_4 \longrightarrow Rb$, the anomalous part of the birefringence decreases gradually and very significantly (by a factor of 12).

An analysis of the changes in the birefringence during the phase transitions in three representatives of the $A_2MO_2F_4$ family revealed a large difference in their values. However, the sequence of two phase transitions in the compounds containing ammonia and atomic cations $(NH_4)_2WO_2F_4$ and $Rb_2MoO_2F_4$ allows us to assume that the initial cause of the structural PTs is a gradual ordering of the octahedral groups. The partial or complete ordering of ligands O and F due to hydrogen bonds formed at T_1 changes the ammonia polarizability, which leads to stronger responses of the physical properties (anomalies in the birefringence and heat capacity) in the ammonia crystals than those in $Rb_2MoO_2F_4$.

ACKNOWLEDGMENTS

This study was supported by the Council on Grants from the President of the Russian Federation for Supporting of Leading Scientific Schools of the Russian Federation (grant NSh-924.2014.2).

REFERENCES

1. A. A. Udovenko and N. M. Laptash, Acta Crystallogr., Sect. B: Struct. Sci. **64**, 645 (2008).
2. V. D. Fokina, E. V. Bogdanov, E. I. Pogorel'tsev, V. S. Bondarev, I. N. Flerov, and N. M. Laptash, Phys. Solid State **52** (1), 158 (2010).
3. A. A. Udovenko, A. D. Vasiliev, and N. M. Laptash, Acta Crystallogr., Sect. B: Struct. Sci. **66**, 34 (2010).
4. V. S. Sergienko, M. A. Porai-Koshits, and T. S. Khodashova, Zh. Strukt. Khim. **13** (3), 461 (1972).
5. S. V. Mel'nikova, V. D. Fokina, and N. M. Laptash, Phys. Solid State **48** (1), 117 (2006).
6. S. V. Mel'nikova and N. M. Laptash, Phys. Solid State **50** (3), 511 (2008).
7. E. V. Bogdanov, A. D. Vasil'ev, I. N. Flerov, and N. M. Laptash, Phys. Solid State **53** (2), 303 (2011).
8. E. V. Bogdanov, E. I. Pogorel'tsev, S. V. Mel'nikova, M. V. Gorev, I. N. Flerov, M. S. Molokeev, A. V. Kartashev, A. G. Kocharova, and N. M. Laptash, Phys. Solid State **55** (2), 409 (2013).
9. A. S. Krylov, S. V. Goryainov, N. M. Laptash, A. N. Vtyurin, S. V. Melnikova, and S. N. Krylova, Cryst. Growth Des. **14**, 374 (2014).

Translated by Yu. Ryzhkov